Volume 69, Issue 2, 2025
Journal of Scientific Research
of
The Banaras Hindu University

Variability of the optical and radiative characteristics of aerosols and classification of aerosol types over the Indo-Gangetic Plain during 2008 to 2018

Nabin Sharma[1], Sarvan Kumar[2], Kalpana Patel[1*]

[1]Department of Physics, SRM Institute of Science and Technology, Delhi-NCR Campus, Modinagar, Ghaziabad-201204, ns6153@srmist.edu.in ;

[1]Department of Physics, SRM Institute of Science and Technology, Delhi-NCR Campus, Modinagar, Ghaziabad-201204, kalpnas@srmist.edu.in*

[2]Department of Earth and Planetary Sciences, VBS Purvanchal University, Jaunpur, Uttar Pradesh-222003, sarvanbhaskar07@gmail.com

Abstract: **This study explores aerosol optical and radiative properties using Aerosol Robotic Network (AERONET) data over Kanpur in Indo-Gangetic Plain (IGP). The study examines long-term variations in Angstrom Exponent (AE) and Aerosols Optical Depth (AOD) over Kanpur from January 2008 to December 2018. The current study shows monthly high values of AOD and AE over Kanpur throughout the monsoon, post-monsoon seasons, and pre-monsoon seasons with low values. Seasonal variation shows AOD with high values for 340 nm in comparison to 440 nm and 500 nm. Reverse trends for AE were observed under the same wavelength comparison. Result-wise, 99.47% contribution of aerosols above Kanpur is from biomass burning/urban-industrial. The Single scattering albedo, Asymmetry parameter, and Refractive Index show the dominancy of coarse mode particles for pre-monsoon and monsoon seasons and fine mode particles for winter and post-monsoon seasons. The results from the HYSPLIT back trajectory for Kanpur show that the dominant air masses over Kanpur consist mostly of polluted dust particles originating from the Thar Desert and Middle East regions.**

Index Terms: **AERONET, Angstrom Exponent, albedo, Single scattering, HYSPLIT.**

I. INTRODUCTION

The Earth's energy balance is directly affected through aerosol particles by radiation absorption and scattering. In addition, they have a significant effect on public health and environmental issues (S. Kumar et al., 2012). They may also affect the micro-physical processes of clouds, which can have an indirect effect on the radiative balance. According to (Myhre, 2009), more data about aerosol features including optical characteristics, chemical composition, and size distribution particularly light absorption properties is necessary for investigations into aerosol impacts on climate. Globally, the climate is significantly influenced by aerosols in the atmosphere because of their direct, indirect, and semi-direct interactions with terrestrial and solar radiation. According to their size distribution, aerosols can be classified as fine or coarse mode particles, given that they originate from a variety of sources and endure a vast array of production mechanisms and mingling processes (Xia et al., 2013). Precursor gases (including SO_2, NO_2, and volatile organic compounds) fragment during the formation of fine-mode aerosols; smaller particles coagulate; and vapors condense during combustion. In contrast, both natural and anthropogenic processes result in the direct emission of course-mode aerosols into the atmosphere. Aerosols vary in their physical and optical characteristics, as well as their chemical compositions, over time and space due to their distinct aging and formation processes. Because of these fluctuations, the climate system is impacted on a regional and global scale through a variety of radiative effects (Kaskaoutis et al., 2009; Volkova et al., 2018). Aerosol impact on the climate must be quantified, and it is crucial to identify the various types and sources of aerosols, those produced naturally or by humans, by monitoring their spatio-temporal fluctuation.

The analysis of aerosol optical properties focuses exclusively on their significant effect on the Earth's climate and their importance in atmospheric predictions. Satellite remote sensing and ground-based techniques are the primary sources to measure the aerosols in the atmosphere. Long-term ground-based monitoring plays an important role in measuring the optical properties of aerosols. The AERONET network examines the

characteristics of aerosols through ground-based measurements. The ground-based radiometric measurements conducted in South Asia have provided valuable information on the significant variations in aerosol concentration. The optical properties of aerosols have not been investigated for forecasting climate change at a global level (Hansen et al., 2000). The precise and comprehensive thought of the optical properties of aerosols is still limited(Allen et al., 2011). The utilization of the AE in conjunction with the aerosol optical depth enables the investigation of aerosol particle growth and size (Boselli et al., 2012). According to (Russell et al., 2002), the single scattering albedo (SSA) plays an important role in establishing a relationship between satellite-measured radiance and AOD, affecting the influence of aerosols on radiation. Northern India is home to the Indo-Gangetic Plain (IGP), a massive river basin that ranks among the world's biggest. Across the southern foothills of the Himalayas in South Asia, it stretches from the north-west limits of the Indian subcontinent to the Bay of Bengal in the east. The presence of large rivers like the Indus, Ganges, and Brahmaputra makes the IGP a very fertile area for farming (Tiwari et al., 2013). Population expansion, increased urbanization, and increasing traffic densities are some of the causes that have contributed to a dramatic rise in aerosol loading in the IGP. The visibility and air quality in the region are negatively affected by this. Aerosols in this region are produced by a variety of sources, some of which are naturally occurring and others of which are induced by humans. These sources show significant seasonal and annual changes (Gao et al., 2011). Furthermore, during periods of high pollution, aerosol radiative forcing may reveal atmospheric features (Che et al., 2014).

Numerous studies indicate that the IGP experiences a higher concentration of aerosol particles compared to other parts of India consistently throughout the year. These studies additionally suggest a variation in the sources and kinds of aerosols in the IGP region depending on the season. Mineral dust is transported across large distances throughout the pre-monsoon season, and local dust rises due to strong, deportation causing a high concentration of aerosols. Pre-monsoon dust storms may transport huge amounts of dust from barren and desert areas in Africa, Arabia, and Rajasthan to the IGP. The significant presence of aerosols has a considerable impact on the activities of monsoons occurring over the IGP. The combination of air pollutants and dust particles in arid air leads to the formation of hazy conditions over the IGP during the pre-monsoon season. Both direct and diffuse solar radiation can be detected and measured using various ground-based measurement networks, including AERONET, PHOTONS, AEROCAN, CARSNET, and SKYNET. The purpose of ground data is to verify the accuracy of satellite findings (Kleidman et al., 2005; Xia et al., 2007) and determine the optical characteristics of aerosols (Dubovik et al., 2002; Holben et al., 2001; Kim et al., 2004). Apart from various studies over IGP still a long-term trend of optical and radiative properties of aerosols and their classification is not properly understood. The systematic study of the atmospheric factors in the Kanpur region is necessary for understanding the long-term trends and characteristics of different types of aerosols. To fill the above gap the present study is initiated. Moreover, the aerosol-monsoon climate might be disrupted in the north Indian region and the Himalayan foothills and slopes due to the radiative effects of aerosols. As the outcome of crop burning throughout the post-monsoon season in Punjab, Haryana, and the western part of Uttar Pradesh the IGP region experiences significant aerosol activity.

The objective of the present study is to examine the long-term ground-based data acquired from the Kanpur AERONET station between 2008 and 2018 and investigate the variability in optical and radiative characteristics of aerosols, with a particular emphasis on the aerosol optical depth (AOD), Angstrom exponent (AE), aerosol volume size distribution (VSD), single scattering albedo (SSA), asymmetry parameter (ASY), and refractive index (RI). Based on the correlation between AOD and AE we have classified different types of aerosols observed over Kanpur. The backward trajectory analysis utilized the hybrid Single-Particle Lagrangian Integrated Trajectories (HYSPLIT) model, a commonly used model in atmospheric research for transport and dispersion, to determine the origin of different categories of aerosols.

II. Method & Materials

A. Study Area

The Indo-Gangetic Plain (IGP), which contains much of the northern parts of India, plays a significant role in agriculture, industry, and economic activity. It also has the nation's highest aerosol loading (Roy, 2021). The City of Kanpur lies in the Indo-Gangetic region at the center of the subcontinent. There are a number of industries in Kanpur, including leather, textiles, and chemicals (Gupta, 2008). Using the WHO Ambient Air Quality Database for 2018, it was named the most polluted city in the world for $PM_{2.5}$ concentrations. Kanpur has a population of 34,703,334 as per the 2011 census. Many different sources are responsible for the pollutants that are found in the air. These sources include emissions from vehicles, pollution from factories, and crop burning in the surrounding (Murari et al., 2015). The area is characterized by a humid subtropical climate, meaning that the summers are long and hot, whereas the winters are moderate and short. Additionally, dust storms and summer monsoon activity are characterized by this region (Sivaprasad & Babu, 2014).

B. Ground-based data (Aerosol robotic network; AERONET)

This ground-based station network was designed to evaluate the performance of the sun/sky photometer CIMEL CE-318 by NASA (Holben et al., 1998). It measures different types and quantities of aerosols, as well as water vapor (precipitated water), in different atmospheric regions. It is situated over the rooftop of the Indian Institute of Technology (IIT), Kanpur (26.4499° N,

80.3319° E, and 142 m above mean sea level). Direct solar radiation and diffuse sky radiance are both detected by the CIMEL radiometer, which operates throughout the spectral range of 340 to 1020 nm. The spectral channels at eight different wavelengths (340, 380, 440, 500, 670, 870, 940, and 1020 nm) are used for measuring solar direct radiation, while the spectral channels at four different wavelengths (440, 670, 870, and 1020 nm) have been used for measuring aerosol optical characteristics. In the AERONET network, aerosol parameters are classified into three categories: 1.0 for unscreened data, 1.5 for cloud-screened and quality-controlled data, and 2.0 for quality-guaranteed data, which is used in the present study.

III. Results and Discussions

A. Yearly and monthly variations in Aerosol Optical Depth (AOD) and Angstrom Exponent (AE) over Kanpur

Fig.1 illustrates the Annual variations of AOD (340, 440, and 500 nm) and AE with monthly mean and standard deviation (SD) wavelengths 340-440 nm,440-870 nm, and 500-870 nm at Kanpur station in the period of January 2008 – December 2018.

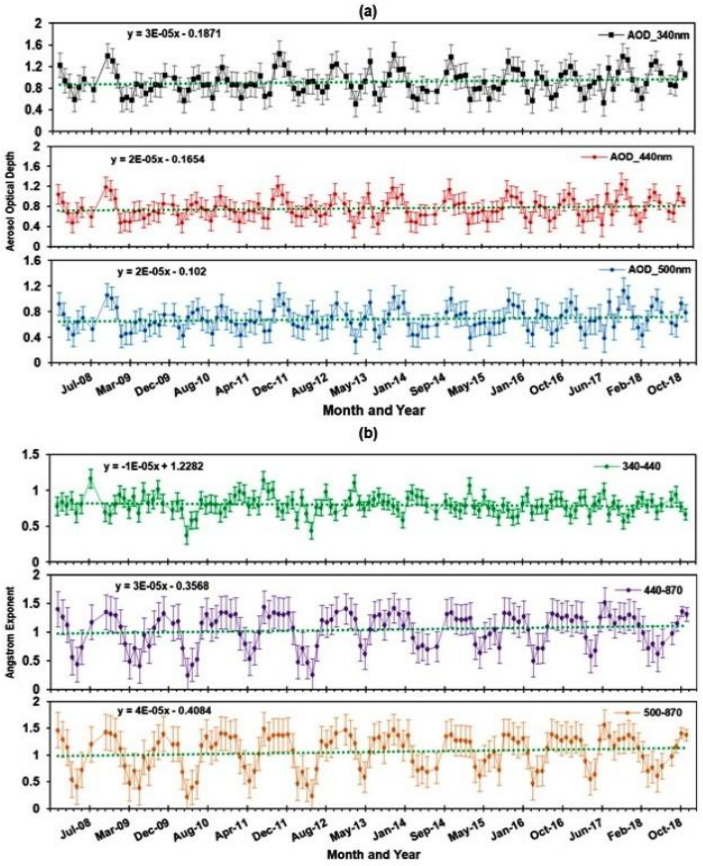

Fig. 1. (a) Annual Changes in (a) Aerosol Optical Depth (AOD) and (b) Angstrom Exponent (AE) with mean ± SD at Kanpur station from January 2008 to December 2018 for specific wavelength ranges (340-440 nm, 440-870 nm, and 500-870 nm).

Fig. 1 (a), shows that the peak value of AOD for wavelengths 500 nm and 440 nm were found 1.13 ± 0.22 and 1.25 ± 0.23 respectively in November 2017 whereas the AOD value at 340 nm was 1.44 ± 0.25 in November 2011. It is also observed that the minimum value of AOD at wavelengths 500 nm, 440 nm, and 340 nm were 0.33 ± 0.10, 0.38 ± 0.08, and 0.51 ± 0.06 respectively in March 2013. The results suggest that the AOD at 340 nm is showing a small increase in trend (3 ×10-5 per month), whereas the AOD at both 440 nm and 500 nm is showing a small increasing trend (2 × 10^{-5} per month). From Fig. 1 (b), it is observed that the highest monthly average value of AE for wavelengths 500 – 870 nm and 440-870 nm was found 1.56 ± 0.33 and 1.51 ± 0.31 respectively in July 2017 whereas AE values for 340 – 440 nm was 1.16 ± 0.1 in Aug 2008. It was observed that the lowest values of AE at wavelengths 340 –440 nm, 440 – 870 nm, and 500 – 870 nm were 0.37 ± 0.06, 0.24 ± 0.09, and 0.21 ± 0.10 during April 2010. A small decreasing trend of AE (-1×10^{-5} per month) is observed at 340 – 440 nm, while small increasing trends of 3×10^{-5} and 4×10^{-5} per month are observed between 440 – 870 nm and 500 – 870 nm respectively. The observed trends in AE suggest a spectral variation in aerosol properties. The small decrease in AE from 340–440 nm might indicate a reduction in smaller or UV-active aerosols (Y. Li et al., 2024). Conversely, the increases from 440–870 nm and 500–870 nm suggest either an increase in larger aerosol particles or a shift in aerosol composition, affecting longer wavelengths more prominently (Kapoor et al., 2023; Yang et al., 2024). In this study, the peak values of monthly AOD and AE for certain wavelengths were found during post-monsoon and monsoon respectively. This occurred because burning biomass, industrial activity, and vehicle emissions may all lead to an increase in aerosol emissions during the monsoon and post-monsoon seasons. Peak levels during these seasons might result from the large contribution of these aerosols to the AOD and AE values (Alam et al., 2010; Tiwari et al., 2013). Seasons defined by the monsoon and post-monsoon bring with them distinct weather patterns such as higher humidity, precipitation, and altered wind patterns. Higher AOD and AE values may result from these meteorological conditions' effects on the aerosols' concentration, dispersion, and transit in the atmosphere (Burton et al., 2012). The minimum values of monthly AOD and AE were recorded in pre-monsoon. This occurred due to the commencement of rainfall in several places during the pre-monsoon seasons. Wet deposition is a mechanism by which precipitation efficiently eliminates particles from the atmosphere. Raindrops function as scavengers, purging aerosol particles from the atmosphere and reducing the concentration of raindrops, resulting in decreased AOD and AE values (Z. Li et al., 2010; Solanki & Pathak, 2023). When (Solanki & Pathak, 2023) studied the optical characteristics of the aerosol in the semi-arid and dusty region of Jaipur they found that the pre-monsoon and post-monsoon seasons had maximum and minimum values of AE and AOD, respectively. Consequently, the results of this study are consistent with those of earlier investigations.

In Fig. 2, the monthly mean AOD with standard deviation for AOD 500 nm, AOD 440 nm, AOD 340 nm, and AE 500 – 870 nm, AE 440 – 870 nm, and AE 340 – 440 nm at Kanpur station during 2015 are shown. The year 2015 was chosen for the monthly variation of AOD over Kanpur due to the abundant and consistent accessibility of data for the whole year. The highest AOD values were found at a wavelength of 340 nm in November and then reduced gradually as the wavelength increased.

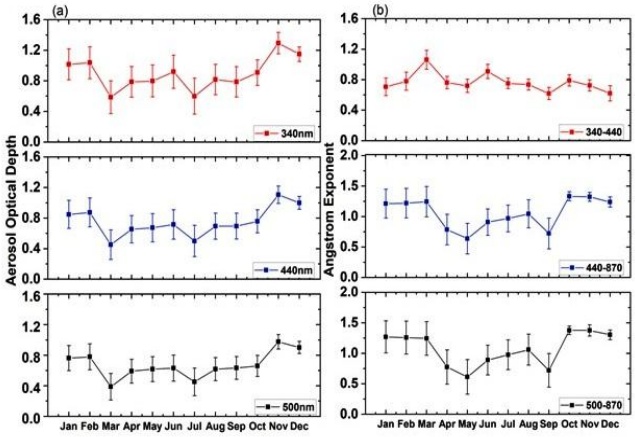

Fig.2. The monthly variations with mean ± SD in the (a) Aerosol Optical Depth (340 nm, 440 nm, and 500 nm) (b) Angstrom Exponent (340-440 nm, 440-870 nm, and 500-870 nm) at Kanpur station.

Conversely, the lowest AOD values were recorded at 500 nm in March and increased gradually as the wavelength decreased (Fig. 2 (a)). Aerosols scatter shorter wavelengths, like blue and UV light, more effectively than longer wavelengths, like red and infrared, which is why this occurred. Thus, the scattering effect diminishes with wavelength, resulting drop in AOD (Sharma et al., 2010; Tiwari et al., 2013). According to the findings shown in Fig. 2(b), it can be noticed that the maximum AE value was found for the wavelength range of 500-870 nm. As the wavelength reduced, the AE value gradually decreased as well. Conversely, the lowest AE value was observed for the wavelength range of 340-440 nm. As the wavelength increased the AE value gradually increased as well. Smaller aerosol particles including fine dust, smoke, and pollutants scatter light more at shorter wavelengths. Higher scattering at shorter wavelengths reduces the peak value of the AE (Deep et al., 2021; Yan et al., 2008). The lowest and highest levels of AE are recorded in October and September accordingly (Fig. 2 (b)). The best agreement has been found between our results and the results of the earlier studies (Deep et al., 2021; Solanki & Pathak, 2023; Soni et al., 2014).

B. Seasonal variation in AOD and AE at distinct wavelengths

Fig. 3 shows the seasonal variation in AOD and AE, together with mean and Standard Deviation, of the three distinct wavelengths over the Kanpur station from January 2008 to December 2018. The highest values of AOD340 nm, AOD440 nm, and AOD500 nm with standard deviation were found to be 1.16±0.18, 0.96±0.15, and 0.84±0.13, respectively, throughout the post-monsoon period (Fig. 3(a)). This occurrence is a result of the regular drop in rainfall during the post-monsoon periods, which leads to a decrease in the process of moist scavenging of aerosols from the atmosphere. Consequently, aerosols remain in the atmosphere for extended durations, hence leading to elevated AOD values (Deep et al., 2021). However, the lowest values of AOD340 nm, AOD440 nm, and AOD500 nm were recorded as 0.77±0.16, 0.63±0.06, and 0.57±0.07, respectively, during the Monsoon season (Fig. 3 a).

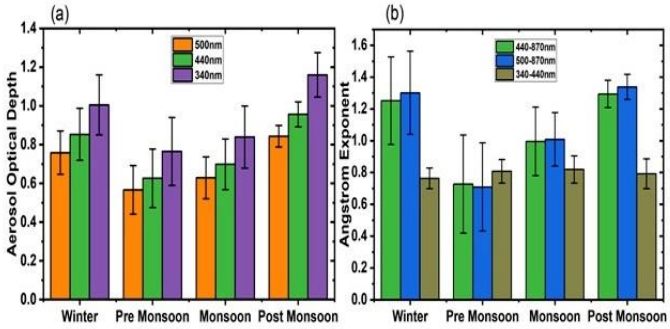

Fig.3. Seasonal variations in (a) Aerosol Optical Depth (AOD) and (b) Angstrom Exponent (AE) with mean ± Standard Deviation for three different wavelengths at Kanpur station from January 2008 to December 2018.

Heavy rainfall is a defining feature of monsoon seasons. Rainfall removes aerosol particles from the atmosphere, acting as a natural "cleanser" for the atmosphere. Consequently, during the monsoon season, the number of aerosols in the atmosphere falls, which lowers AOD levels (R. Kumar et al., 2014). Fig. 3 (b), illustrates that the highest values of AE with standard deviation (SD) for wavelengths 500 – 870 nm and 440 – 870 nm, were 1.34±0.28, and 1.29±0.31, respectively during post-monsoon whereas it was 0.82±0.09 for the wavelength 340 – 440 nm during monsoon. Because of increased humidity, convective activity, and local sources like burning biomass and urban pollutants, post-monsoon seasons usually see greater aerosol loading. A larger percentage of smaller aerosol particles in the atmosphere due to increased aerosol loading produces higher AE values at lower wavelengths because they scatter light more effectively at shorter wavelengths (Helin et al., 2021). The pre-monsoon season had the lowest values of AE for wavelengths 500–870 nm and 440–870 nm, which were 0.37±0.13 and 0.40±0.14, respectively, whereas the winter saw the lowest values of AE for wavelengths 340–440 nm, which was 0.59±0.15 as shown in Fig. 3(b). Shorter wavelengths of light may be less scattered and absorbed because of the density drop in the aerosol. Furthermore, air pollutants and particulate matter may behave differently as temperatures drop, which might lower their concentration and, in turn, their impact on AE (Tiwari et al., 2016; Viswanatha Vachaspati et al., 2018a).

C. Classification of Aerosol Types over Kanpur

The relationship between AOD and AE to comprehend the main categories of aerosols in the atmosphere. The Indo-Gangetic

plains (Rupakheti et al., 2018), the African subcontinent (Boiyo et al., 2019), Southeast Asia (Khan et al., 2019), Central Asia (Rupakheti et al., 2019), and various other locations in China (Shaheen et al., 2019), India (S. Kumar et al., 2023; Patel & Singh, 2023a), Pakistan (Alam et al., 2016; Iftikhar et al., 2018) and Nepal (Rupakheti et al., 2018) have all been studied using this methodology, including atmospheric conditions (such as haze occurrences), various kinds of emissions, and geographical locations. In order to distinguish between different kinds of aerosols, we have taken the same threshold values for AOD and AE as those used in previous studies (Rupakheti et al., 2019). They are classified as the Continental Clean (CC) aerosol type when the AOD is less than 0.2 and the AE is greater than 1.0; the Clean Marine (CM) aerosol type when the AOD is less than 0.2 and the AE is less than 0.7; the Biomass burning/Urban-industrial (BUI) aerosol type when the AOD is greater than 0.3 and the AE is greater than 1.0; and the Desert Dust (DD) aerosol type when the AOD is greater than 0.6 and the AE is less than 0.7. Aerosols that do not meet any of the abovementioned requirements are classified as the Mixed (MX) aerosol type. The scatter plots in Fig. 4 depict the correlation between AOD and AE, indicating the existence of many aerosol types in Kanpur.

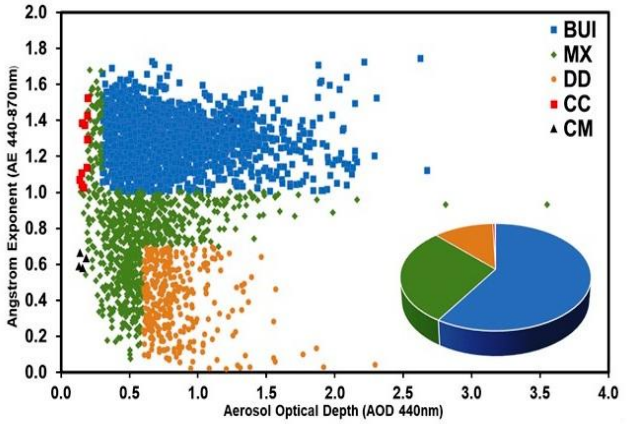

Fig.4. The relationship between the aerosol optical depth (AOD) and the angstrom exponent (AE) is used to categorize various types of aerosols observed over Kanpur. The pie chart shows how different aerosol types are distributed.

During the study period, the most prominent aerosol types were BUI (58.86%), MX (28.86%), and DD (11.75%) which account for 99.47% of the total aerosols. In the atmosphere, CC (0.38%) and CM (0.15%) aerosols are present in smaller quantities. Since the study area is geographically separated from the sea and Fig.5 presents a description of the seasonal distribution of various types of aerosols. BUI is the most significant type of aerosol that occurs during post-monsoon (93.88%), winter (85.52%), and monsoon (49.63%). During the post-monsoon period, the BUI type of aerosol was the predominant kind of aerosol, and this is because of the transportation of intensive crop residue burning emissions across the northwest IGP (Jethva et al., 2019; Ramachandran et al., 2015). Ocean, CC and CM aerosol levels are low (Filonchyk et al., 2021). In all seasons, MX aerosols were observed in large amounts, with the most (56.42%) in pre-monsoon and the least (6.13%) in post-monsoon. Different-sized particles formed from various sources are mixed to form MX aerosols (Boiyo et al., 2019; K. R. Kumar et al., 2018). Kanpur is the most densely inhabited and commercial city in India. Pré-monsoon (24.22%), monsoon (18.16%), and winter (0.82%) were the times when the DD type of aerosol was detected; it was not present during the post-monsoon. It is due to the winds carrying dust from local industries and automobiles, as well as dust from streets and

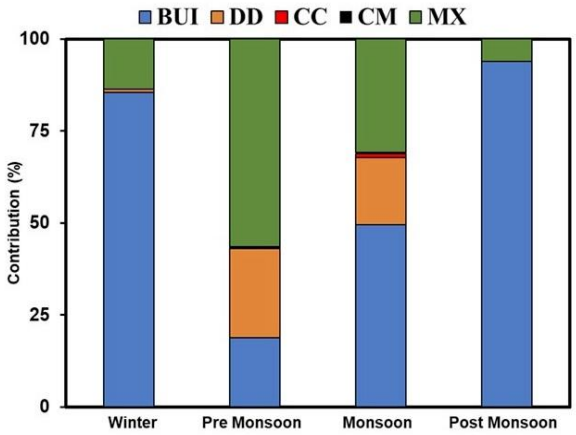

Fig.5.Seasonal distribution of different types of aerosols and their percentage contributions.

deserts during the pre-monsoon and monsoon seasons (Dey et al., 2005; Singh et al., 2004). With just a fraction below 2% in all seasons, CM and CC aerosol types made the smallest contributions. Based on the results, it can be concluded that all types of aerosols played a role in different seasons at different levels of influence. Each aerosol type contributes to the seasonal climate in a different way based on the type of climate, air mass movement, and atmospheric chemical and physical processes (Kumar et al., 2018).

D. Study of Seasonal aerosol volume size distribution (VSD)

A sun/sky photometer evaluates the optical characteristics of aerosols, which are significantly affected by the distribution of columnar aerosol and particle size variations. Coarse particles are defined as particles with a size more than 0.6 µm, whilst fine particles are those with a size less than 0.6 µm. A total of 22 distinct radii, ranging from 0.05 to 15 µm, are used by the AERONET Kanpur station to accurately measure the aerosol volume size distribution (VSD). The results obtained in $\mu m^3/\mu m^2$ units measured the volume of entire aerosol particles volume in the vertical air column. Analysis of VSD data reveals bimodal log-normal distributions for the seasonal mean VSD, seen in Fig. 6. It was noted that fine-mode aerosols were prevalent in each season, equivalent to findings in other Eastern European cities like Moscow (Chubarova et al., 2011) and Kyiv (Milinevsky et al., 2014).

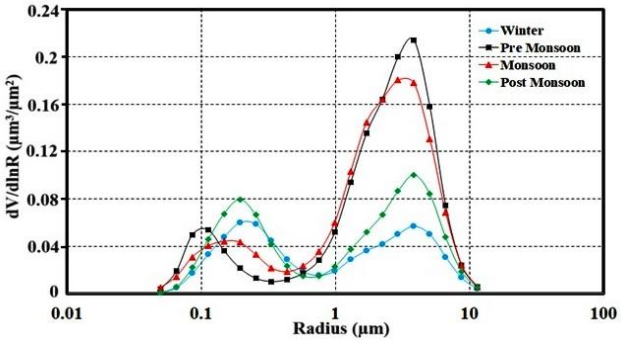

Fig.6.Variations in the aerosol volume size distribution over Kanpur during different seasons.

According to Fig. 6, the highest percentages of fine particles were found in the monsoon, post-monsoon, and winter seasons. The volume concentrations within a radius of 0.18μm were 0.059 $\mu m^3/\mu m^2$, 0.044 $\mu m^3/\mu m^2$, and 0.079 $\mu m^3/\mu m^2$ respectively for each season. A common source of aerosol formation is indicated by practically similar volume distributions. The high relative humidity and high temperature give rise to an increment in fine particles during winter and post-monsoon (Filonchyk et al., 2021; Priyadharshini et al., 2018; Yu et al., 2017). In contrast, VSD during the pre-monsoon season is distinct from VSD throughout other seasons. During the pre-monsoon season, the VSD distribution in fine aerosols was measured to be 0.053 $\mu m^3/\mu m^2$. The maximum radius of the fine mode decreased to 0.11μm in comparison to other seasons. It appears that the increased mode radius of fine particles can be attributed to the formation of hygroscopic aerosols under pre-monsoon circumstances, which are characterized by higher relative humidity. (Gobbi et al., 2007).Coarse particles have an important part in the overall volume concentration. Agricultural activities, wind erosion, and unfavorable weather conditions may create mineral dust aerosols that have a notable impact on aerosol properties.VSD in the coarse mode exhibited distinct variations across different seasons. In the pre-monsoon and monsoon seasons, the VSD values were noticeably higher, measuring 0.213 $\mu m^3/\mu m^2$ and 0.180 $\mu m^3/\mu m^2$ respectively. In contrast, the VSD values were diminished throughout the winter and post-monsoon seasons, measuring 0.100 $\mu m^3/\mu m^2$ and 0.056 $\mu m^3/\mu m^2$ respectively. These measurements were taken within a radius of 5.06 μm. Ploughing and crop harvesting are two examples of agricultural activities that contributed to the higher values that were seen throughout the pre-monsoon and post-monsoon seasons. In comparison with the pre-monsoon volume concentration, the monsoon value is low due to a large amount of precipitation in the region, which may help to remove coarse particles (Patel & Singh, 2023b; Viswanatha Vachaspati et al., 2018b).

E. Study of the seasonal spectral variation of the AERONET-retrieved parameters over Kanpur

Fig. 7 (a) illustrates the seasonal fluctuations of Single Scattering Albedo (SSA) over Kanpur. The aerosol's direct radiative forcing by considering the scattering factor and the extinction coefficient is calculated by using SSA. Understanding the geographical distribution of SSA is crucial during emergencies like forest fires. Various biomass combustion products may combine to form aerosol particles that possess significant absorption capabilities due to their organic and black carbon composition. Through its capability to absorb solar radiation, carbon plays an important role in warming the atmosphere of the Earth. Aerosols that scatter more are indicated by higher SSA values (≈1), whilst those that scatter less are indicated by lower SSA values (Dubovik et al., 2002). In order to determine whether an aerosol will be cooling or heating, the SSA is a key factor (Andrews et al., 2017). Fig. 7(a), shows that the values of SSA at wavelength 675 nm for the single scattering albedo are seasonal averages following an order: monsoon (0.95±0.03) > post-monsoon (0.92±0.01) > pre-monsoon (0.91±0.03) > winter (0.90±0.02).

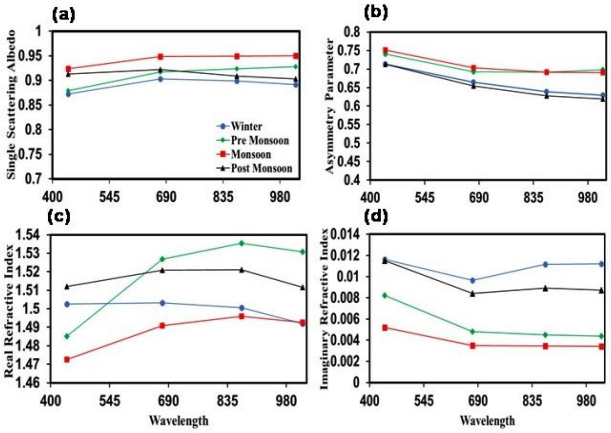

Fig.7.Seasonality of (a) single scattering albedo (SSA), (b) asymmetry parameter (ASY), (c) real refractive index (RRI), and (d) imaginary refractive index (IRI) in Kanpur based on AERONET data.

It is dominant that urban aerosols absorb solar radiation during the winter months over Kanpur, resulting in SSA that is lower at longer wavelengths since these urban aerosols do not interact with solar radiation as much as at shorter wavelengths. Coarse particles, mostly dust, are thought to constitute the predominant component throughout the pre-monsoon and monsoon seasons. In contrast, the SSA remains rather constant across different wavelengths throughout the post-monsoon period. (Singh et al., 2004). It was suggested that dust aerosols (Alam et al., 2011; Iftikhar et al., 2018; Tiwari et al., 2015) contributed to the same spectral characteristics of SSA in the IGP region (here, values that rise from visible to near-infrared wavelengths).

Fig. 7(b) illustrates the seasonal fluctuations of the Asymmetry parameter (ASY) over Kanpur. Light scattering after interaction with aerosol particles is characterized by ASY. This parameter determines how much aerosol radiative forcing is caused by the size and composition of particles. For totally forward scattered radiation, the ASY values fall within the range of +1, whereas for totally backward scattered radiation, they fall within the range of

-1 (Dubovik et al., 2002). Since the sizes of aerosols are equivalent to the wavelengths of interacting radiation, the asymmetry ratio changes in accordance with the wavelength. Throughout the complete study period, the average value of ASY_{675} was 0.68±0.02. The seasonal values were determined, monsoon (0.70±0.01) > pre-monsoon (0.69±0.02) > winter (0.66±0.01)> post-monsoon (0.65±0.01). In Delhi, ASY_{675} values for various aerosol kinds were reported: 0.71±0.01 for polluted dust, 0.68±0.02 for polluted continental, 0.66±0.02 for most importantly Black carbon, and 0.68±0.03 for most importantly organic carbon.(Srivastava et al., 2014). The human activity that occurred during the cold season led to a reduction in the amount of ASY that was present at high wavelengths, which resulted in the increased presence of fine particles.(Andrews et al., 2006).

The Refractive Index (RI) of aerosol particles provides details about their nature and chemical composition. The RI consists of both real and imaginary parts, known as RRI and IRI, respectively. Fig.7(c) illustrates the seasonal fluctuations of the real refractive index (RRI) over Kanpur. The RRI provides ideas about the absorbing and scattering properties of aerosols by relating hygroscopic growth and atmospheric humidity. Fig. 7(d) illustrates the seasonal fluctuations of the imaginary refractive index (IRI) over Kanpur. The higher RRI indicates that aerosol particles scatter more effectively while the higher IRI indicates that they absorb more (Singh et al., 2004). As shown in Fig 7(c and d), RRI and IRI exhibit varying spectral variations with wavelength. RRI (and IRI) at 675 nm were found as 1.50±0.02 (0.0096±0.0015) throughout winter, 1.53±0.01 (0.0047±0.0014) throughout pre-monsoon, 1.49±0.03 (0.0034±0.0014) throughout monsoon and 1.53±0.01 (0.0084±0.0017) throughout post-monsoon. During all seasons, RRI increases from 440nm to 675nm, with a decrease at 1020nm and an increase at 870nm (except during the winter). In Winter, high RRI values at shorter wavelengths may indicate that fine-mode dust aerosols are present, while lower values at longer wavelengths show coarse-mode dust aerosols (Adesina et al., 2017). The IRI demonstrates the aerosols' moisture-absorbing capacity. Winter values are higher due to higher concentrations of black carbon aerosols, which also result in lower SSA values. Scattering coarse-mode dust aerosols are present during monsoon and pre-monsoon because of the low IRI in these seasons. (Filonchyk et al., 2021).

F. Source identification using Back Trajectories with the HYSPLIT Model

The five-day back trajectories of the HYSPLIT model are shown in Fig. 8 on the days when the observed AOD over Kanpur is at its maximum. The several long-range transport mechanisms are shown by the backward trajectories in terms of both height and distance. The HYSPLIT model was used to calculate 5-day back trajectories at altitudes of 500, 1000, and 1500 m. The trajectories were used to identify the source of air pollutants and examine how transportation patterns influence the levels of these pollutants in Kanpur, India. As part of the research period, the days that had the greatest values of AOD (>2) for the Kanpur region were chosen. The study analysed the back trajectories on specific dates (19 January 2008, 05 June 2010, 30 October 2012, 03 November 2014, 24 December 2016, and 30 December 2018) over Kanpur obtained through the Hybrid Single-Particle Lagrangian Integrated Trajectories (HYSPLIT) model structured by the National Oceanic and Atmospheric Administration at three different heights. The model can be found at the following website: https://www.ready.noaa.gov/HYSPLIT.php. Fig. 8 illustrates that the air mass at low and medium elevations arises from the continental area. It seems like the air mass is being brought over Kanpur from faraway places like the Sahara Desert, the Arabian Peninsula, and the Thar Desert from January to December. Regardless of natural variations in meteorological circumstances and aerosol transport, the two metrics (i.e., AOD and AE) over Kanpur show very moderate and consistent variations.

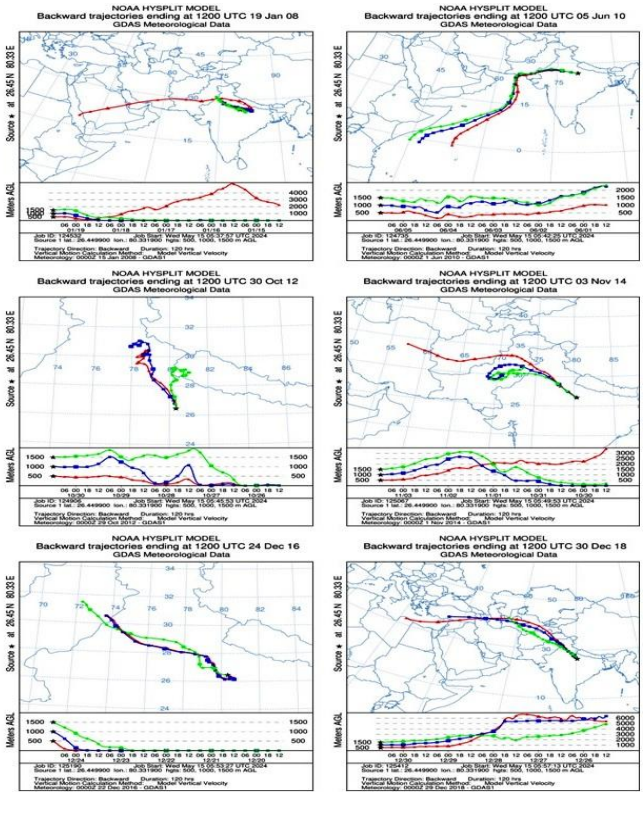

Fig.8. The five-day back trajectories of the HYSPLIT model on certain days in different seasons with the highest AOD over Kanpur.

Because seasonal wind patterns fluctuate, different types of aerosols might be carried to the observation locations from different parts of the world. Examples include ocean salt, desert dust, and man-made aerosols originating from biomass and urban-industrial activities. Air mass trajectories show that the Thar Desert is the main origin of dust when the higher air mass comes from the Persian and Oman Gulf areas. Aerosol sources similar to those over the Indo-Gangetic Plain were identified by (Gautam et

al., 2010). Dominant air masses over Kanpur consist mostly of polluted dust particles originating from the Thar Desert and Middle East regions, according to Tiwari et al. (2015). During the pre-monsoon season, larger particles such as sea salt and dust become more prominent, traveling longer distances and causing significant variations in latitudinal movements, leading to instability in Kanpur (Tiwari et al., 2013).

CONCLUSION

The current study shows considerable variations in atmospheric parameters over the Kanpur region. It focuses primarily on trends in the Angstrom Exponent (AE) and Aerosols Optical Depth (AOD) over the Kanpur between January 2008 and December 2018, classifying the different types of aerosols based on the correlation between AOD and AE, thereby, different aerosol particles are observed over the Kanpur region, allowing the radiation budget and its impact on Earth's climate to be computed. As a consequence of this, the availability of further ground-based observations and the recognition of aerosols that are based on geographic areas is of the utmost vital significance. The uncertainty, limitations, and possible results of the present research must be emphasized. The HYSPLIT model may provide, within certain limitations, a critical outline of the pollutant transit paths to the target location. The current research observed that the monthly AOD and AE peak values over Kanpur at specified wavelengths occurred during the post-monsoon and monsoon, respectively, whereas the monthly AOD and AE low values were only seen during the pre-monsoon. During the seasonal investigation, it was revealed that the fraction of AOD trend was greater for wavelengths of 340 nm in comparison to 440 nm and 500 nm wavelengths. Conversely, the pattern for AE was the opposite, with lower values reported for the same wavelengths. The dominant form of aerosol seen throughout the post-monsoon, winter, and monsoon seasons was BUI, accounting for 93.88%, 85.52%, and 49.63% respectively. The values of VSD were notably greater in the pre-monsoon and monsoon seasons, whereas they were notably lower in the remaining two seasons (winter and post-monsoon seasons). Throughout pre-monsoon and monsoon seasons, fine particles, mostly dust, are assumed to be the main component. Nonetheless, throughout the post-monsoon phase, the SSA is rather stable at various wavelengths. Throughout the whole duration of the investigation, the mean value of ASY675 was 0.68±0.02. The HYSPLIT model utilized trajectory analysis to point out the source of air masses over Kanpur. Dominant air masses over Kanpur consist mostly of polluted dust particles originating from the Thar Desert and Middle East regions.

ACKNOWLEDGMENTS

The authors are thankful to the NASA AERONET team for providing aerosol data, as well as the NOAA ARL Laboratory for HYSPLIT Back Trajectories. One of the authors Sarvan Kumar is Thankful to the University Grants Commission for providing funds through the BSR UGC Start-Up Research grant (No.F.30-573/2021(BSR); Dated:15 June 2022).

REFERENCES

Adesina, A. J., Piketh, S., Kanike, R. K., & Venkataraman, S. (2017). Characteristics of columnar aerosol optical and microphysical properties retrieved from the sun photometer and its impact on radiative forcing over Skukuza (South Africa) during 1999–2010. *Environmental Science and Pollution Research*, *24*(19), 16160–16171. https://doi.org/10.1007/s11356-017-9211-2

Alam, K., Iqbal, M. J., Blaschke, T., Qureshi, S., & Khan, G. (2010). Monitoring spatio-temporal variations in aerosols and aerosol-cloud interactions over Pakistan using MODIS data. *Advances in Space Research*, *46*(9), 1162–1176. https://doi.org/10.1016/j.asr.2010.06.025

Alam, K., Shaheen, K., Blaschke, T., Chishtie, F., Khan, H. U., & Haq, B. S. (2016). Classification of aerosols in an urban environment on the basis of optical measurements. *Aerosol and Air Quality Research*, *16*(10), 2535–2549. https://doi.org/10.4209/aaqr.2016.06.0219

Alam, K., Trautmann, T., & Blaschke, T. (2011). Aerosol optical properties and radiative forcing over mega-city Karachi. *Atmospheric Research*, *101*(3), 773–782. https://doi.org/10.1016/j.atmosres.2011.05.007

Allen, G., Coe, H., Clarke, A., Bretherton, C., Wood, R., Abel, S. J., Barrett, P., Brown, P., George, R., Freitag, S., McNaughton, C., Howell, S., Shank, L., Kapustin, V., Brekhovskikh, V., Kleinman, L., Lee, Y. N., Springston, S., Toniazzo, T., … Chand, D. (2011). South East Pacific atmospheric composition and variability sampled along 20° S during VOCALS-REx. *Atmospheric Chemistry and Physics*, *11*(11), 5237–5262. https://doi.org/10.5194/acp-11-5237-2011

Andrews, E., Ogren, J. A., Kinne, S., & Samset, B. (2017). Comparison of AOD, AAOD and column single scattering albedo from AERONET retrievals and in situ profiling measurements. *Atmospheric Chemistry and Physics*, *17*(9), 6041–6072. https://doi.org/10.5194/acp-17-6041-2017

Andrews, E., Sheridan, P. J., Fiebig, M., McComiskey, A., Ogren, J. A., Arnott, P., Covert, D., Elleman, R., Gasparini, R., Collins, D., Jonsson, H., Schmid, B., & Wang, J. (2006). Comparison of methods for deriving aerosol asymmetry parameter. *Journal of Geophysical Research Atmospheres*, *111*(5), 1–16. https://doi.org/10.1029/2004JD005734

Boiyo, R., Kumar, K. R., Zhao, T., & Guo, J. (2019). A 10-Year Record of Aerosol Optical Properties and Radiative Forcing Over Three Environmentally Distinct AERONET Sites in Kenya, East Africa. *Journal of Geophysical Research: Atmospheres*, *124*(3), 1596–1617. https://doi.org/10.1029/2018JD029461

Boselli, A., Caggiano, R., Cornacchia, C., Madonna, F., Mona, L., Macchiato, M., Pappalardo, G., & Trippetta, S. (2012). Multi year sun-photometer measurements for aerosol

characterization in a Central Mediterranean site. *Atmospheric Research*, *104–105*, 98–110. https://doi.org/10.1016/j.atmosres.2011.08.002

Burton, S. P., Ferrare, R. A., Hostetler, C. A., Hair, J. W., Rogers, R. R., Obland, M. D., Butler, C. F., Cook, A. L., Harper, D. B., & Froyd, K. D. (2012). Aerosol classification using airborne High Spectral Resolution Lidar measurements-methodology and examples. *Atmospheric Measurement Techniques*, *5*(1), 73–98. https://doi.org/10.5194/amt-5-73-2012

Che, H., Xia, X., Zhu, J., Li, Z., Dubovik, O., Holben, B., Goloub, P., Chen, H., Estelles, V., Cuevas-Agulló, E., Blarel, L., Wang, H., Zhao, H., Zhang, X., Wang, Y., Sun, J., Tao, R., Zhang, X., & Shi, G. (2014). Column aerosol optical properties and aerosol radiative forcing during a serious haze-fog month over North China Plain in 2013 based on ground-based sunphotometer measurements. *Atmospheric Chemistry and Physics*, *14*(4), 2125–2138. https://doi.org/10.5194/acp-14-2125-2014

Chubarova, N., Smirnov, A., & Holben, B. (2011). Aerosol Properties in Moscow According To 10 Years of Aeronet Measurements At the Meteorological Observatory of Moscow State University. *Geography, Environment, Sustainability*, *4*(1), 19–32. https://doi.org/10.24057/2071-9388-2011-4-1-19-32

Deep, A., Pandey, C. P., Nandan, H., Singh, N., Yadav, G., Joshi, P. C., Purohit, K. D., & Bhatt, S. C. (2021). Aerosols optical depth and Ångström exponent over different regions in Garhwal Himalaya, India. *Environmental Monitoring and Assessment*, *193*(6). https://doi.org/10.1007/s10661-021-09048-4

Dey, S., Tripathi, S. N., Singh, R. P., & Holben, B. N. (2005). Seasonal variability of the aerosol parameters over Kanpur, an urban site in Indo-Gangetic basin. *Advances in Space Research*, *36*(5), 778–782. https://doi.org/10.1016/j.asr.2005.06.040

Dubovik, O., Holben, B., Eck, T. F., Smirnov, A., Kaufman, Y. J., King, M. D., Tanré, D., & Slutsker, I. (2002). Variability of absorption and optical properties of key aerosol types observed in worldwide locations. *Journal of the Atmospheric Sciences*, *59*(3), 590–608. https://doi.org/10.1175/1520-0469(2002)059%3C0590%3AVOAAOP%3E2.0.C

Filonchyk, M., Peterson, M., Yan, H., Yang, S., & Chaikovsky, A. (2021). Columnar optical characteristics and radiative properties of aerosols of the AERONET site in Minsk, Belarus. *Atmospheric Environment*, *249*(January), 118237. https://doi.org/10.1016/j.atmosenv.2021.118237

Gao, L., Jia, G., Zhang, R., Che, H., Fu, C., Wang, T., Zhang, M., Jiang, H., & Yan, P. (2011). Visual range trends in the Yangtze River Delta Region of China, 1981-2005. *Journal of the Air and Waste Management Association*, *61*(8), 843–849. https://doi.org/10.3155/1047-3289.61.8.843

Gautam, R., Hsu, N. C., & Lau, K. M. (2010). Premonsoon aerosol characterization and radiative effects over the Indo-Gangetic plains: Implications for regional climate warming. *Journal of Geophysical Research Atmospheres*, *115*(17), 1–15. https://doi.org/10.1029/2010JD013819

Gobbi, G. P., Kaufman, Y. J., Koren, I., & Eck, T. F. (2007). Classification of aerosol properties derived from AERONET direct sun data. *Atmospheric Chemistry and Physics*, *7*(2), 453–458. https://doi.org/10.5194/acp-7-453-2007

Gupta, U. (2008). Valuation of urban air pollution: A case study of Kanpur City in India. *Environmental and Resource Economics*, *41*(3), 315–326. https://doi.org/10.1007/s10640-008-9193-0

Hansen, J., Sato, M., Ruedy, R., Lacis, A., & Oinas, V. (2000). Global warming in the twenty-first century: An alternative scenario. *Proceedings of the National Academy of Sciences of the United States of America*, *97*(18), 9875–9880. https://doi.org/10.1073/pnas.170278997

Helin, A., Virkkula, A., Backman, J., Pirjola, L., Sippula, O., Aakko-Saksa, P., Väätäinen, S., Mylläri, F., Järvinen, A., Bloss, M., Aurela, M., Jakobi, G., Karjalainen, P., Zimmermann, R., Jokiniemi, J., Saarikoski, S., Tissari, J., Rönkkö, T., Niemi, J. V., & Timonen, H. (2021). Variation of Absorption Ångström Exponent in Aerosols From Different Emission Sources. *Journal of Geophysical Research: Atmospheres*, *126*(10), 1–21. https://doi.org/10.1029/2020JD034094

Holben, B. N., Eck, T. F., Slutsker, I., Tanré, D., Buis, J. P., Setzer, A., Vermote, E., Reagan, J. A., Kaufman, Y. J., Nakajima, T., Lavenu, F., Jankowiak, I., & Smirnov, A. (1998). AERONET - A federated instrument network and data archive for aerosol characterization. *Remote Sensing of Environment*, *66*(1), 1–16. https://doi.org/10.1016/S0034-4257(98)00031-5

Holben, B. N., Tanré, D., Smirnov, A., Eck, T. F., Slutsker, I., Abuhassan, N., Newcomb, W. W., Schafer, J. S., Chatenet, B., Lavenu, F., Kaufman, Y. J., Vande Castle, J., Setzer, A., Markham, B., Clark, D., Frouin, R., Halthore, R., Karneli, A., O'Neill, N. T., … Zibordi, G. (2001). An emerging ground-based aerosol climatology: Aerosol optical depth from AERONET. *Journal of Geophysical Research Atmospheres*, *106*(D11), 12067–12097. https://doi.org/10.1029/2001JD900014

Iftikhar, M., Alam, K., Sorooshian, A., Syed, W. A., Bibi, S., & Bibi, H. (2018). Contrasting aerosol optical and radiative properties between dust and urban haze episodes in megacities of Pakistan. *Atmospheric Environment*, *173*, 157–172. https://doi.org/10.1016/j.atmosenv.2017.11.011

Jethva, H., Torres, O., Field, R. D., Lyapustin, A., Gautam, R., & Kayetha, V. (2019). Connecting Crop Productivity, Residue Fires, and Air Quality over Northern India. *Scientific Reports*, *9*(1), 1–11. https://doi.org/10.1038/s41598-019-52799-x

Kapoor, T. S., Phuleria, H. C., Sumlin, B., Shetty, N., Anurag, G., Bansal, M., Duhan, S. S., Khan, M. S., Laura, J. S., Manwani, P., Chakrabarty, R. K., & Venkataraman, C.

(2023). Optical Properties and Refractive Index of Wintertime Aerosol at a Highly Polluted North-Indian Site. *Journal of Geophysical Research: Atmospheres*, *128*(14). https://doi.org/10.1029/2022JD038272

Kaskaoutis, D. G., Badarinath, K. V. S., Kharol, S. K., Sharma, A. R., & Kambezidis, H. D. (2009). Variations in the aerosol optical properties and types over the tropical urban site of Hyderabad, India. *Journal of Geophysical Research Atmospheres*, *114*(22), 1–20. https://doi.org/10.1029/2009JD012423

Khan, R., Kumar, K. R., & Zhao, T. (2019). The climatology of aerosol optical thickness and radiative effects in Southeast Asia from 18-years of ground-based observations. *Environmental Pollution*, *254*, 113025. https://doi.org/10.1016/j.envpol.2019.113025

Kim, D. H., Sohn, B. J., Nakajima, T., Takamura, T., Takemura, T., Choi, B. C., & Yoon, S. C. (2004). Aerosol optical properties over east Asia determined from ground-based sky radiation measurements. *Journal of Geophysical Research: Atmospheres*, *109*(2), 1–18. https://doi.org/10.1029/2003jd003387

Kleidman, R. G., O'Neill, N. T., Remer, L. A., Kaufman, Y. J., Eck, T. F., Tanré, D., Dubovik, O., & Holben, B. N. (2005). Comparison of moderate resolution imaging spectroradiometer (MODIS) and Aerosol Robotic Network (AERONET) remote-sensing retrievals of aerosol fine mode fraction over ocean. *Journal of Geophysical Research Atmospheres*, *110*(22), 1–6. https://doi.org/10.1029/2005JD005760

Kumar, K. R., Boiyo, R., Madina, A., & Kang, N. (2018). A 13-year climatological study on the variations of aerosol and cloud properties over Kazakhstan from remotely sensed satellite observations. *Journal of Atmospheric and Solar-Terrestrial Physics*, *179*, 55–68. https://doi.org/10.1016/j.jastp.2018.06.014

Kumar, R., Barth, M. C., Pfister, G. G., Naja, M., & Brasseur, G. P. (2014). WRF-Chem simulations of a typical pre-monsoon dust storm in northern India: Influences on aerosol optical properties and radiation budget. *Atmospheric Chemistry and Physics*, *14*(5), 2431–2446. https://doi.org/10.5194/acp-14-2431-2014

Kumar, S., Kumar, S., Singh, A. K., & Singh, R. P. (2012). Seasonal variability of atmospheric aerosol over the North Indian region during 2005-2009. *Advances in Space Research*, *50*(9), 1220–1230. https://doi.org/10.1016/j.asr.2012.06.022

Kumar, S., Singh, N., Singh, R. P., & Siingh, D. (2023). Variability of air quality and aerosol over Indian region during 2003–2012. *Indian Journal of Physics*, *97*(1), 17–23. https://doi.org/10.1007/s12648-022-02375-3

Li, Y., Wang, Q., Zhang, Y., Wang, J., Zhou, B., Tian, J., Liu, H., Liu, S., Ran, W., & Cao, J. (2024). Contributions of different organic compounds to brown carbon light absorption in a river-valley region, China. *Atmospheric Environment*, *335*, 120731. https://doi.org/10.1016/j.atmosenv.2024.120731

Li, Z., Lee, K. H., Wang, Y., Xin, J., & Hao, W. M. (2010). First observation-based estimates of cloud-free aerosol radiative forcing across China. *Journal of Geophysical Research Atmospheres*, *115*(17). https://doi.org/10.1029/2009JD013306

Milinevsky, G., Danylevsky, V., Bovchaliuk, V., Bovchaliuk, A., Goloub, P., Dubovik, O., Kabashnikov, V., Chaikovsky, A., Miatselskaya, N., Mishchenko, M., & Sosonkin, M. (2014). Aerosol seasonal variations over urban-industrial regions in Ukraine according to AERONET and POLDER measurements. *Atmospheric Measurement Techniques*, *7*(5), 1459–1474. https://doi.org/10.5194/amt-7-1459-2014

Murari, V., Kumar, M., Barman, S. C., & Banerjee, T. (2015). Temporal variability of MODIS aerosol optical depth and chemical characterization of airborne particulates in Varanasi, India. *Environmental Science and Pollution Research*, *22*(2), 1329–1343. https://doi.org/10.1007/s11356-014-3418-2

Myhre, G. (2009). Consistency between satellite-derived and modeled estimates of the direct aerosol effect. *Science*, *325*(5937), 187–190. https://doi.org/10.1126/science.1174461

Patel, K., & Singh, A. K. (2023a). Consequences of pre and post confinement on the atmospheric air pollutants during spread of COVID-19 in India. *Indian Journal of Physics*, *97*(2), 319–336. https://doi.org/10.1007/s12648-022-02380-6

Patel, K., & Singh, A. K. (2023b). Consequences of pre and post confinement on the atmospheric air pollutants during spread of COVID-19 in India. *Indian Journal of Physics*, *97*(2), 319–336. https://doi.org/10.1007/s12648-022-02380-6

Priyadharshini, B., Verma, S., Giles, D. M., & Holben, B. N. (2018). Discerning the pre-monsoon urban atmosphere aerosol characteristic and its potential source type remotely sensed by AERONET over the Bengal Gangetic plain. *Environmental Science and Pollution Research*, *25*(22), 22163–22179. https://doi.org/10.1007/s11356-018-2290-x

Ramachandran, S., Kedia, S., & Sheel, V. (2015). Spatiotemporal characteristics of aerosols in India: Observations and model simulations. *Atmospheric Environment*, *116*, 225–244. https://doi.org/10.1016/j.atmosenv.2015.06.015

Roy, M. P. (2021). Comment on "Impact of Shutdown due to COVID-19 Pandemic on Aerosol Characteristics in Kanpur, India." *Journal of Health and Pollution*, *11*(29), 1–2. https://doi.org/10.5696/2156-9614-11.29.210313

Rupakheti, D., Kang, S., Bilal, M., Gong, J., Xia, X., & Cong, Z. (2019). Aerosol optical depth climatology over Central Asian countries based on Aqua-MODIS Collection 6.1 data: Aerosol variations and sources. *Atmospheric Environment*, *207*, 205–214. https://doi.org/10.1016/j.atmosenv.2019.03.020

Rupakheti, D., Kang, S., Rupakheti, M., Cong, Z., Tripathee, L., Panday, A. K., & Holben, B. N. (2018). Observation of optical properties and sources of aerosols at Buddha's

birthplace, Lumbini, Nepal: environmental implications. *Environmental Science and Pollution Research*, *25*(15), 14868–14881. https://doi.org/10.1007/s11356-018-1713-z

Russell, P. B., Redemann, J., Schmid, B., Bergstrom, R. W., Livingston, J. M., McIntosh, D. M., Ramirez, S. A., Hartley, S., Hobbs, P. V., Quinn, P. K., Carrico, C. M., Rood, M. J., Öström, E., Noone, K. J., von Hoyningen-Huene, W., & Remer, L. (2002). Comparison of aerosol single scattering albedos derived by diverse techniques in two North Atlantic experiments. *Journal of the Atmospheric Sciences*, *59*(3 PT 2), 609–619. https://doi.org/10.1175/1520-0469(2002)059<0609:coassa>2.0.co;2

Shaheen, K., Shah, Z., Suo, H. L., Liu, M., Ma, L., Alam, K., Gul, A., Cui, J., Li, C., Wang, Y., Khan, S. A., & Khan, S. B. (2019). Aerosol clustering in an urban environment of Beijing during (2005–2017). *Atmospheric Environment*, *213*(June), 534–547. https://doi.org/10.1016/j.atmosenv.2019.06.027

Sharma, A. R., Kharol, S. K., Badarinath, K. V. S., & Singh, D. (2010). Impact of agriculture crop residue burning on atmospheric aerosol loading - A study over Punjab State, India. *Annales Geophysicae*, *28*(2), 367–379. https://doi.org/10.5194/angeo-28-367-2010

Singh, R. P., Dey, S., Tripathi, S. N., Tare, V., & Holben, B. (2004). Variability of aerosol parameters over Kanpur, northern India. *Journal of Geophysical Research D: Atmospheres*, *109*(23), 1–14. https://doi.org/10.1029/2004JD004966

Sivaprasad, P., & Babu, C. A. (2014). Seasonal variation and classification of aerosols over an inland station in India. *Meteorological Applications*, *21*(2), 241–248. https://doi.org/10.1002/met.1319

Solanki, R., & Pathak, K. (2023). Investigation of the aerosol's optical properties over the dust prevalent semi-arid region at Jaipur, northwestern India. *Environmental Engineering Research*, *29*(1), 220758–0. https://doi.org/10.4491/eer.2022.758

Soni, K., Kapoor, S., Parmar, K. S., & Kaskaoutis, D. G. (2014). Statistical analysis of aerosols over the Gangetic-Himalayan region using ARIMA model based on long-term MODIS observations. *Atmospheric Research*, *149*, 174–192. https://doi.org/10.1016/j.atmosres.2014.05.025

Srivastava, A. K., Yadav, V., Pathak, V., Singh, S., Tiwari, S., Bisht, D. S., & Goloub, P. (2014). Variability in radiative properties of major aerosol types: A year-long study over Delhi-An urban station in Indo-Gangetic Basin. *Science of the Total Environment*, *473–474*, 659–666. https://doi.org/10.1016/j.scitotenv.2013.12.064

Tiwari, S., Srivastava, A. K., & Singh, A. K. (2013). Heterogeneity in pre-monsoon aerosol characteristics over the Indo-Gangetic Basin. *Atmospheric Environment*, *77*, 738–747. https://doi.org/10.1016/j.atmosenv.2013.05.035

Tiwari, S., Srivastava, A. K., Singh, A. K., & Singh, S. (2015). Identification of aerosol types over Indo-Gangetic Basin: implications to optical properties and associated radiative forcing. *Environmental Science and Pollution Research*, *22*(16), 12246–12260. https://doi.org/10.1007/s11356-015-4495-6

Tiwari, S., Tiwari, S., Hopke, P. K., Attri, S. D., Soni, V. K., & Singh, A. K. (2016). Variability in optical properties of atmospheric aerosols and their frequency distribution over a mega city "New Delhi," India. *Environmental Science and Pollution Research*, *23*(9), 8781–8793. https://doi.org/10.1007/s11356-016-6060-3

Viswanatha Vachaspati, C., Reshma Begam, G., Nazeer Ahammed, Y., Raghavendra Kumar, K., & Reddy, R. R. (2018a). Characterization of aerosol optical properties and model computed radiative forcing over a semi-arid region, Kadapa in India. *Atmospheric Research*, *209*, 36–49. https://doi.org/10.1016/j.atmosres.2018.03.013

Viswanatha Vachaspati, C., Reshma Begam, G., Nazeer Ahammed, Y., Raghavendra Kumar, K., & Reddy, R. R. (2018b). Characterization of aerosol optical properties and model computed radiative forcing over a semi-arid region, Kadapa in India. *Atmospheric Research*, *209*, 36–49. https://doi.org/10.1016/j.atmosres.2018.03.013

Volkova, K. A., Poberovsky, A. V., Timofeev, Y. M., Ionov, D. V., Holben, B. N., Smirnov, A., & Slutsker, I. (2018). Aerosol Optical Characteristics Retrieved from CIMEL Sun Photometer Measurements (AERONET) near St. Petersburg. *Atmospheric and Oceanic Optics*, *31*(6), 635–641. https://doi.org/10.1134/S1024856018060180

Xia, X., Chen, H., Goloub, P., Zong, X., Zhang, W., & Wang, P. (2013). Climatological aspects of aerosol optical properties in North China Plain based on ground and satellite remote-sensing data. *Journal of Quantitative Spectroscopy and Radiative Transfer*, *127*, 12–23. https://doi.org/10.1016/j.jqsrt.2013.06.024

Xia, X., Chen, H., Li, Z., Wang, P., & Wang, J. (2007). Significant reduction of surface solar irradiance induced by aerosols in a suburban region in northeastern China. *Journal of Geophysical Research Atmospheres*, *112*(22), 1–9. https://doi.org/10.1029/2006JD007562

Yan, P., Tang, J., Huang, J., Mao, J. T., Zhou, X. J., Liu, Q., Wang, Z. F., & Zhou, H. G. (2008). The measurement of aerosol optical properties at a rural site in Northern China. *Atmospheric Chemistry and Physics*, *8*(8), 2229–2242. https://doi.org/10.5194/acp-8-2229-2008

Yang, L., Mao, Y., Liao, H., Xie, M., & Zhang, Y. (2024). Direct radiative forcing of light-absorbing carbonaceous aerosols in China. *Atmospheric Research*, *304*, 107396. https://doi.org/10.1016/j.atmosres.2024.107396

Yu, X., Lü, R., Liu, C., Yuan, L., Shao, Y., Zhu, B., & Lei, L. (2017). Seasonal variation of columnar aerosol optical properties and radiative forcing over Beijing, China. *Atmospheric Environment*, *166*, 340–350. https://doi.org/10.1016/j.atmosenv.2017.07.011

***